

Figure S1. Titration of TCR stimulation, related to Figure 1.

A. Naïve CD4⁺ T cells were stimulated with polystyrene beads coated with indicated amounts of α CD3 and 1 μ g/mL of α CD28 for 5 minutes. Mean fluorescence intensity (MFI) of phosphorylated ZAP70, SLP76 and ERK was measured by flow cytometry gating on bead-bound cells. **B.** MFI of ERK phosphorylation at 1 μ g/mL of α CD3 was measured from 0 to 60 minutes. **C.** Frequency of CD69⁺ cells were determined by flow cytometry after 16 hours of TCR stimulation with indicated α CD3 concentrations. Experiments shown are representative of four experiments.

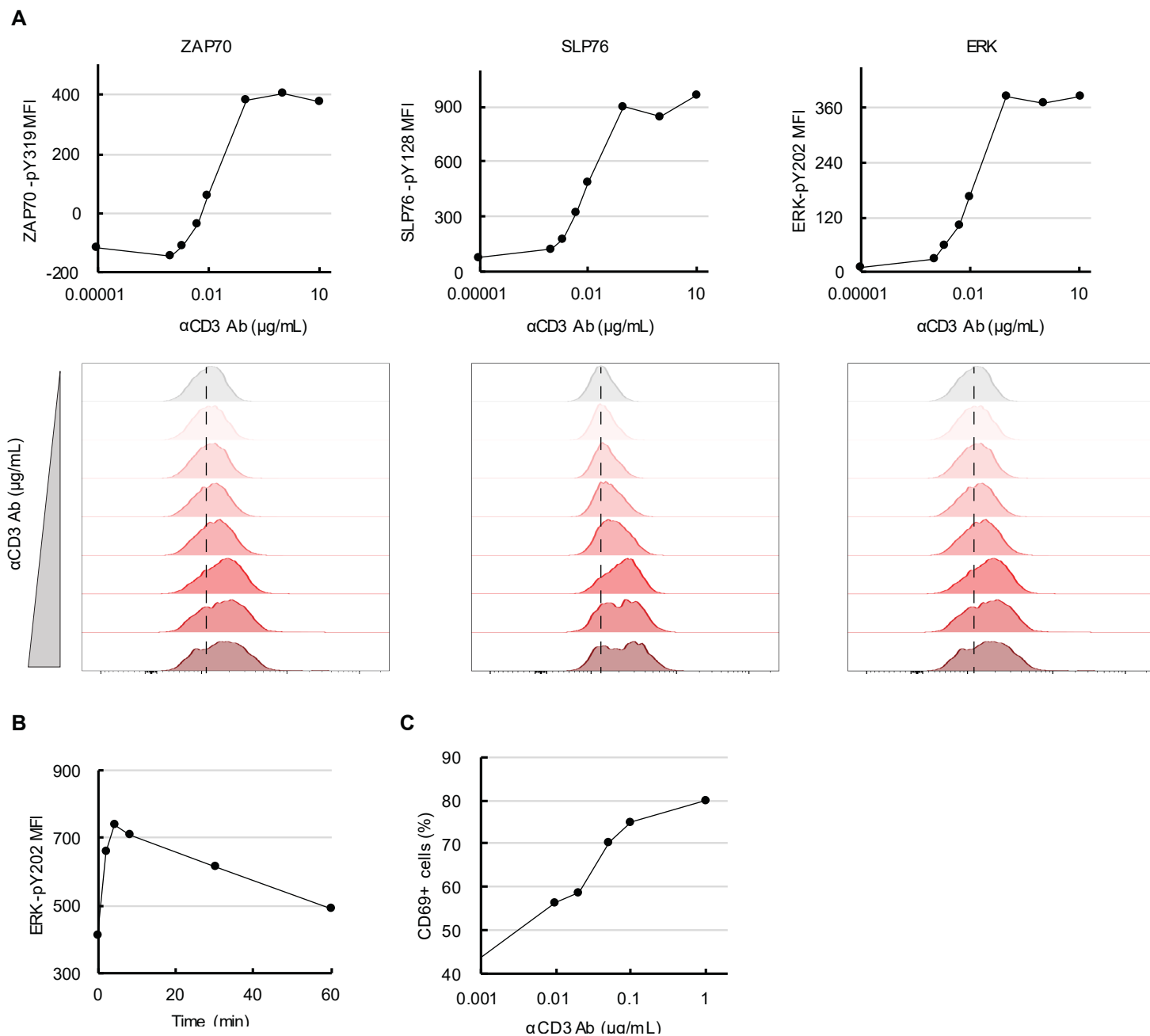


Figure S2. Longitudinal epigenomic and transcriptomic changes induced by TCR stimulation

Naïve CD4⁺ T cells from eight individuals were stimulated with 0.01 (low, square) or 1 µg/mL (median, triangle) αCD3-coated beads and subjected to ATAC-seq and RNA-seq at indicated time points. **A.** Bar graphs show the number of peaks more or less accessible in activated cells compared to base line at each time point. **B.** Total differential peaks between low (left) or high (right) TCR stimulation and baseline are plotted as average log₂ fold-change (logFC) versus log₂ mean reads per peak. Peaks with p-values below 0.05 are indicated in red. **C.** Bar graphs show the number of significantly up- or down-regulated gene transcripts for each time point (p < 0.05). **D.** Total up- or down-regulated gene transcripts in activated cells compared to baseline plotted as logFC versus the average expression.

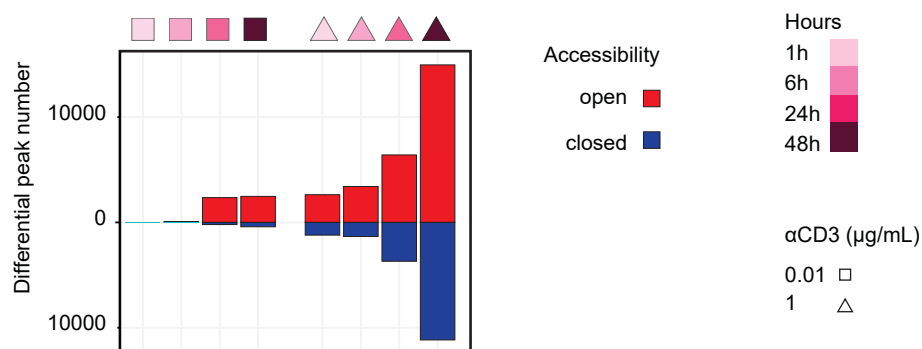
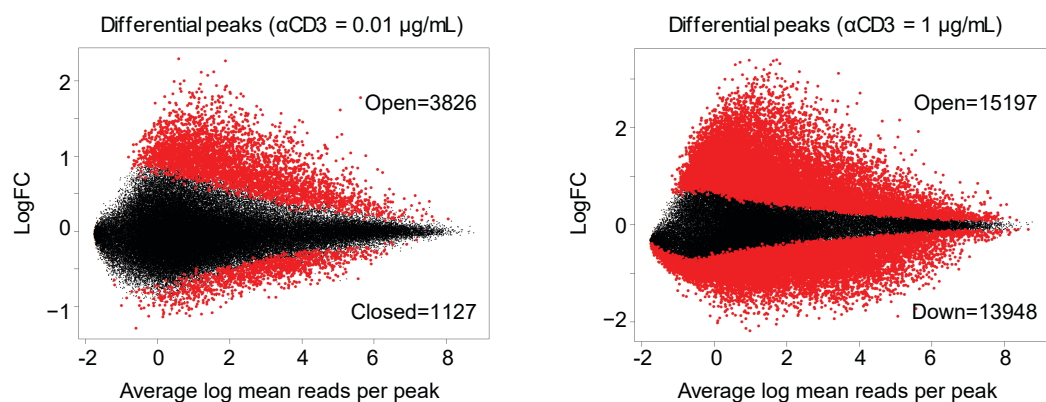
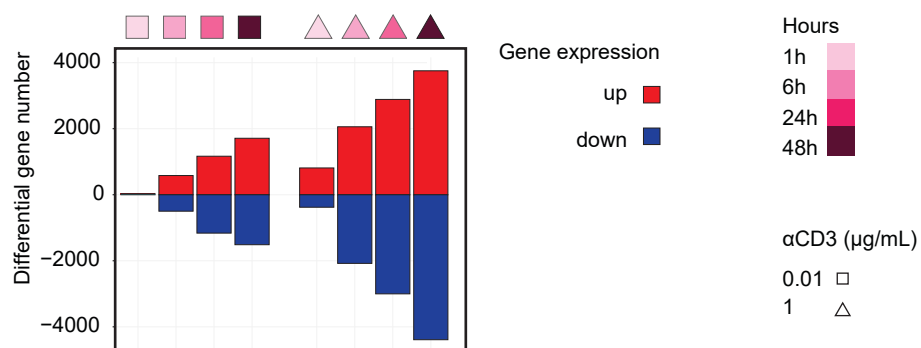
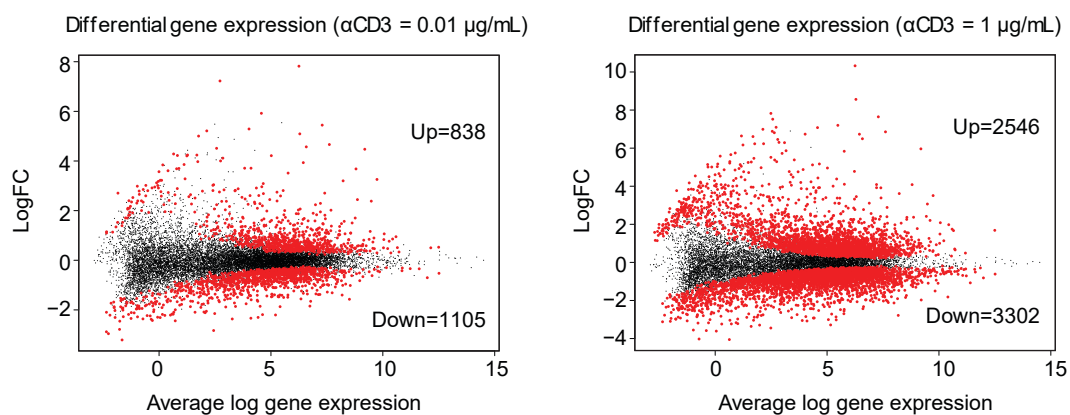
A**B****C****D**

Figure S3. Higher intensity TCR stimulation amplifies age-associated chromatin accessibility differences seen at baseline or with low intensity stimulation

Sites more accessible ($p < 0.05$) in naïve CD4⁺ T cells from young (left) or old (right) adults were identified at baseline and at several time points after TCR stimulation with beads coated with low and medium concentrations of α CD3. Relationships between the three peak sets are shown as Venn diagrams.

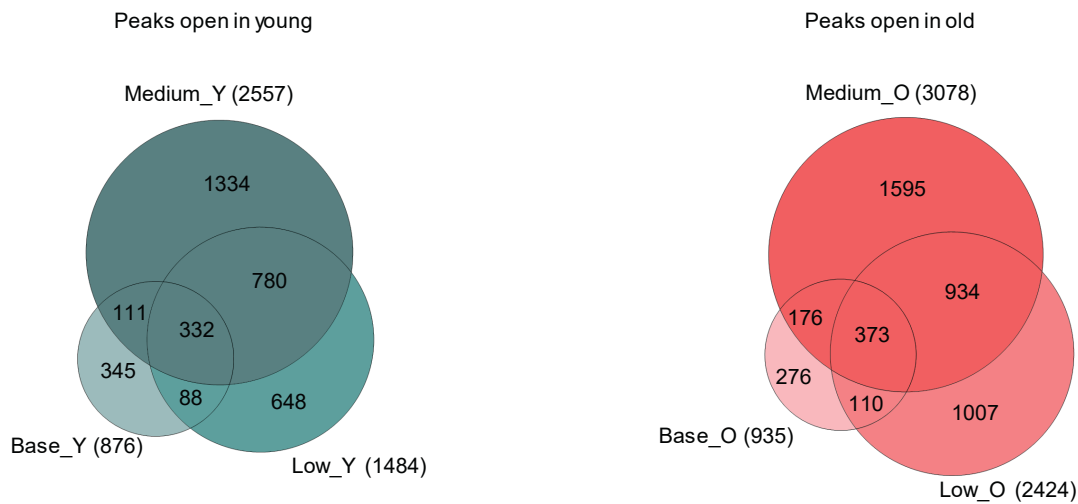
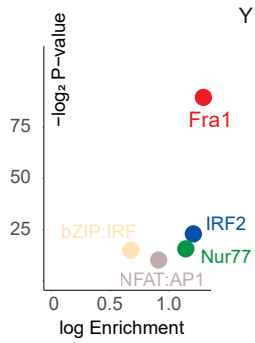


Figure S4. related to Figure 2C. Activation-induced temporal patterns of epigenetic changes in naïve CD4⁺ T cells from young and older adults.

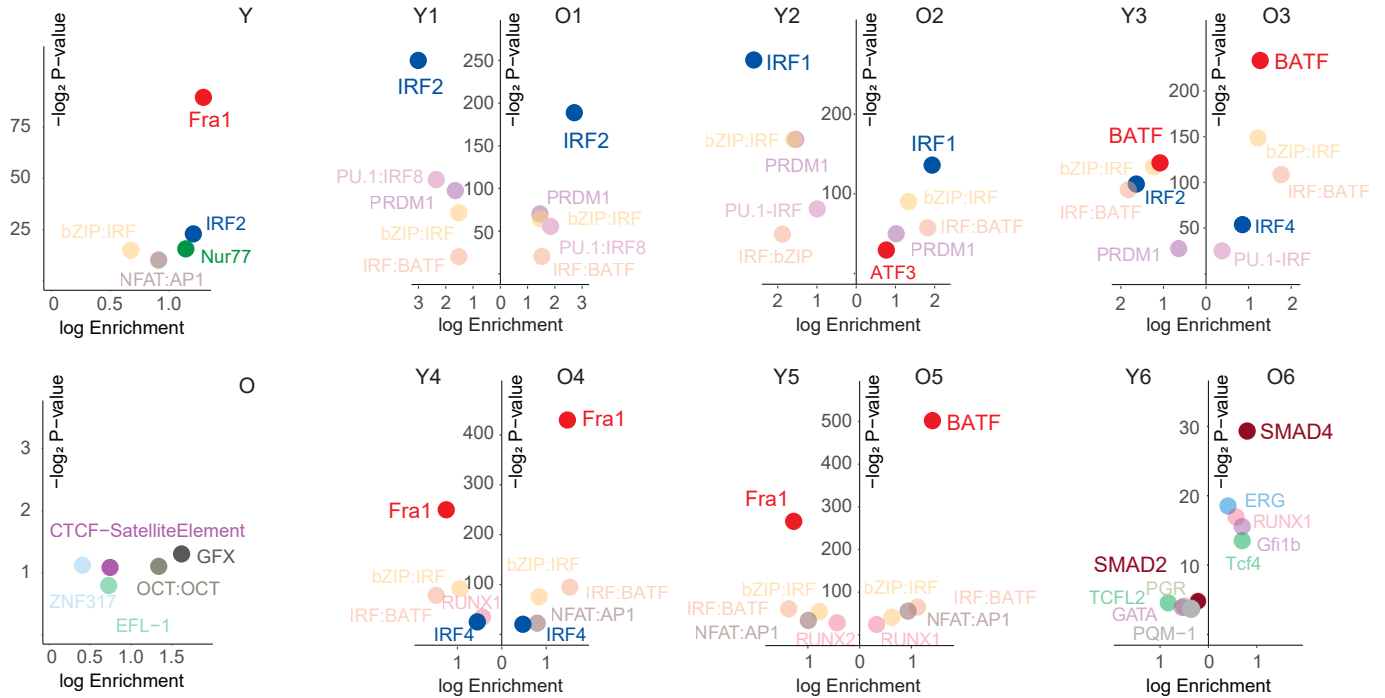
A. Peak sets in clusters with different temporal patterns and membership scores >0.6 as shown in Figure 2C were analyzed for TF motif enrichments by HOMER. Graphs show the fold enrichment (X-axis) in each cluster from young (to the left) and old (to the right) adults plotted vs the significance level (Y-axis). Five TFs with the lowest p-values are shown. **B.** Genes assigned to differentially accessible regulatory sites were examined for significant enrichment in biological pathways. Selected GO terms associated with the different temporal patterns in young (upper panel) and older adults (lower panel) are shown. **C.** Gene expression time course of indicated TFs from RNA-seq data.

A

TF motif enrichment:
Unique clusters

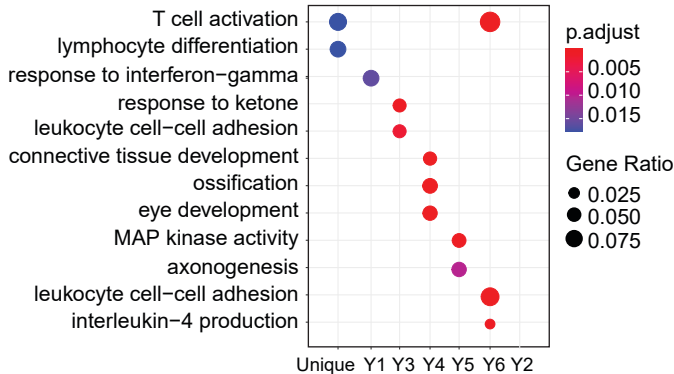


TF motif enrichment: common clusters

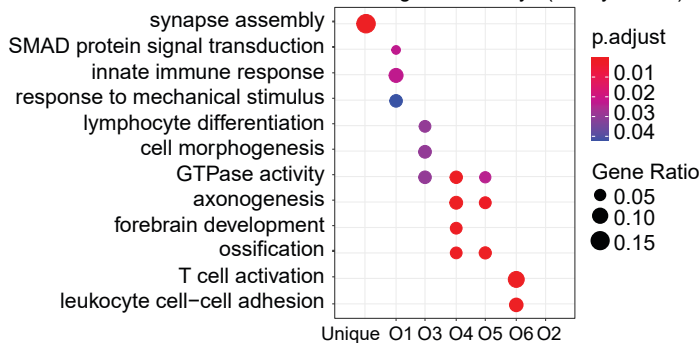


B

GO Biological Pathways (< 35 year old)



GO Biological Pathways (> 65 year old)



C

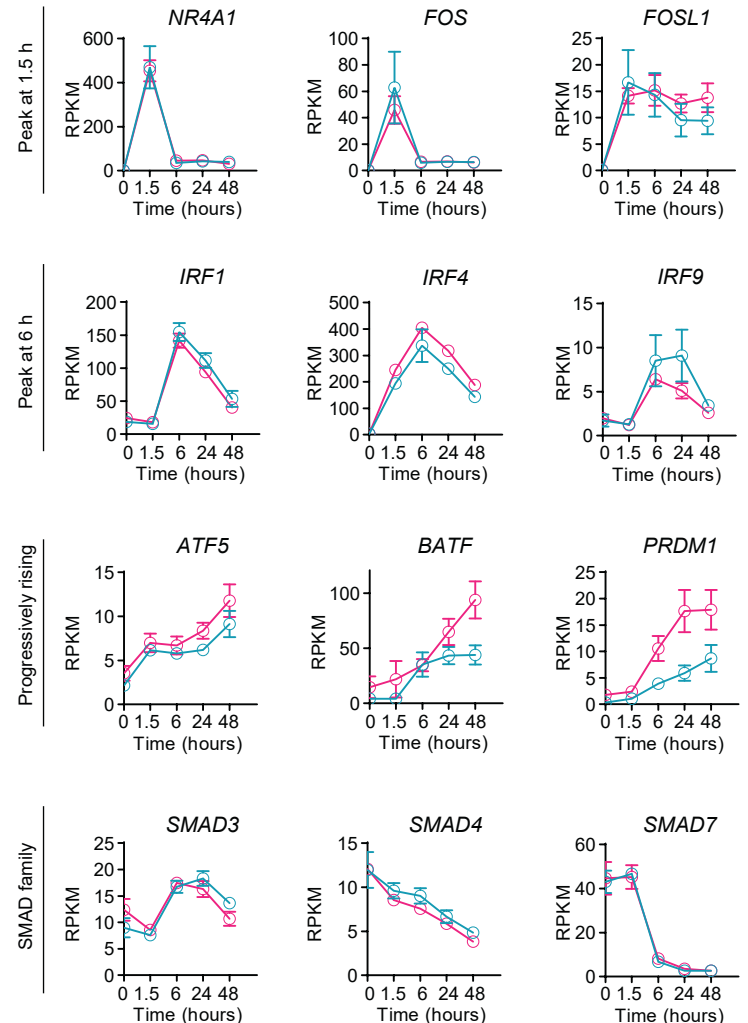


Figure S5, related to Figures 2D and E. Relationship between differential accessibility of regulatory regions and transcriptome

A. Aggregate genome accessibility tracks of representative sites of cluster 7-10 shown in the heat plot in Figure 2D (left panel). Cyan-shaded areas indicate peaks that are more open in young (cyan) compared to older adults (magenta). Transcript data from corresponding genes as determined by RNA-seq (right panel). **B.** LogFC difference of transcripts differentially expressed between young and older adults from 48-hour RNA-seq data is plotted against logFC difference of differential peaks from ATAC-seq data annotated to the same gene at the indicated time point. Data are fitted with linear regression.

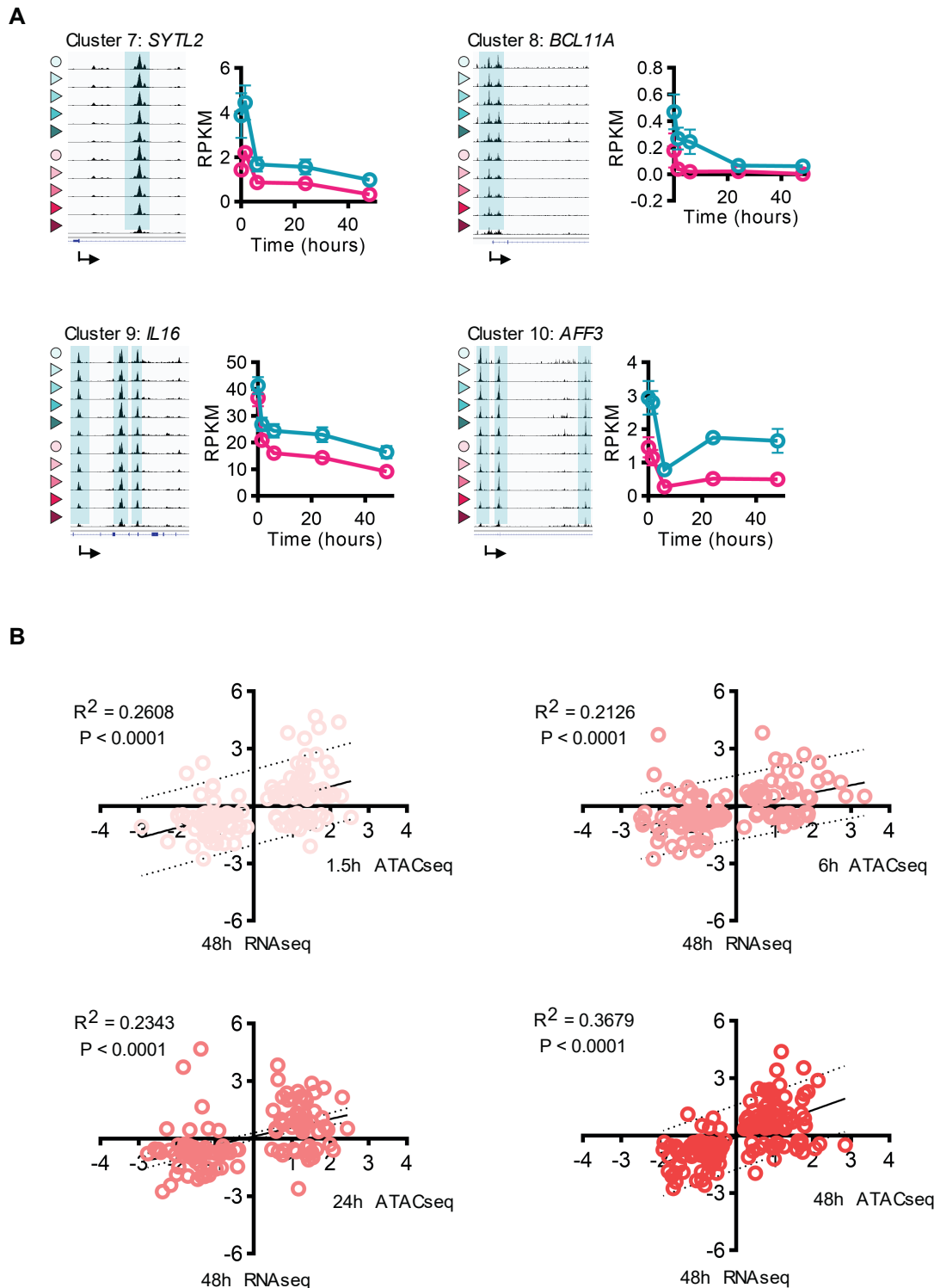


Figure S6, related to Figure 4. Single cell epigenetic and transcriptional analysis of naïve CD4⁺ T cell responses.

Nuclei pooled from unstimulated and activated naïve CD4⁺ T cells were subjected to scATAC- and scRNA-seq. Imputed *CD69* gene expression is projected on the UMAP of scATAC-seq. Clusters of resting and activated cells were distinguished based on containing *CD69*-expressing cells (left panel). UMAP maps of scATAC-seq and scRNA-seq data are shown for activated cells (right panels).

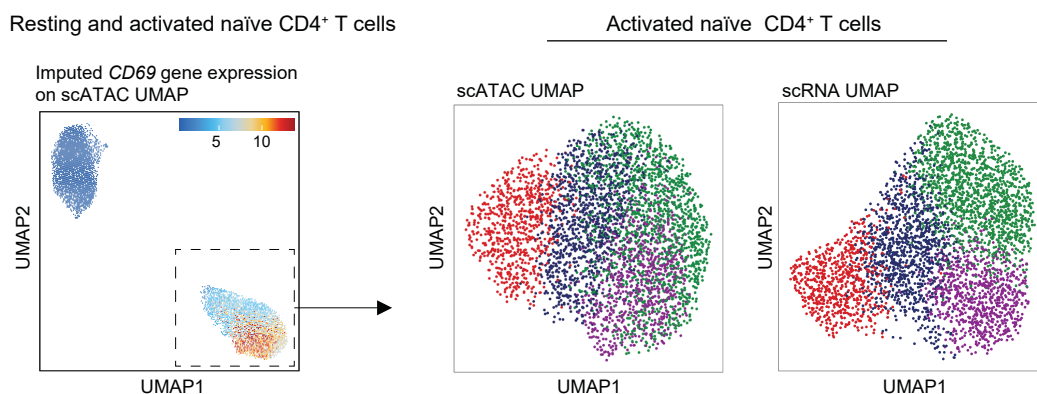


Figure S7. Constitutive expression of the IL-2 receptor on naïve CD4⁺ T cells from older individuals.

A. Gating strategy for naïve CD4⁺ T cells. **B.** *IL2RA* gene expression was quantified in unstimulated naïve CD4⁺ T cells from 10 young and 12 older adults. **C.** CD25 was stained on resting naïve CD4⁺ T cells from 12 young and 10 older adults. Data from B and C were analyzed with unpaired t-test. ** $p < 0.01$.

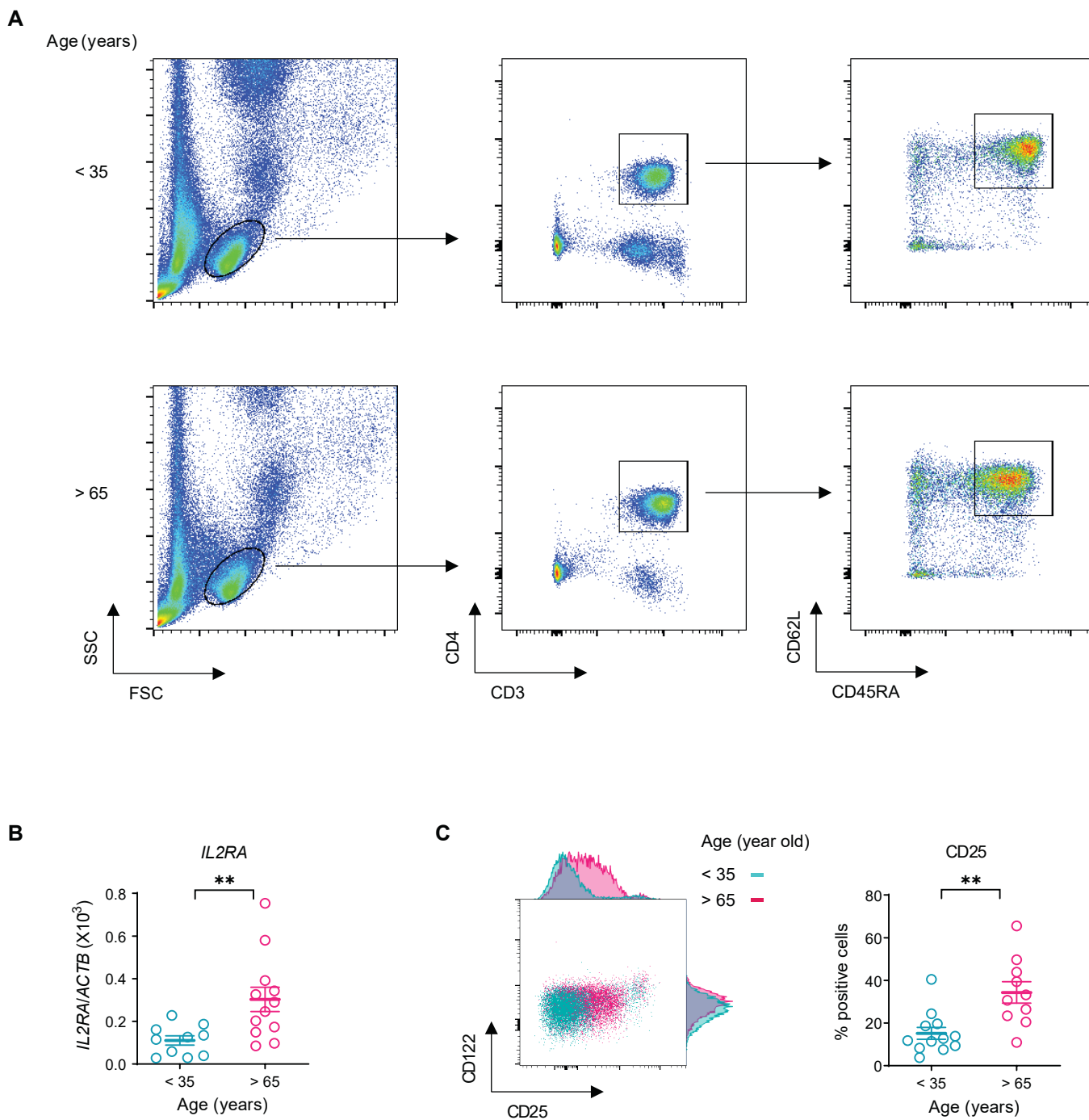
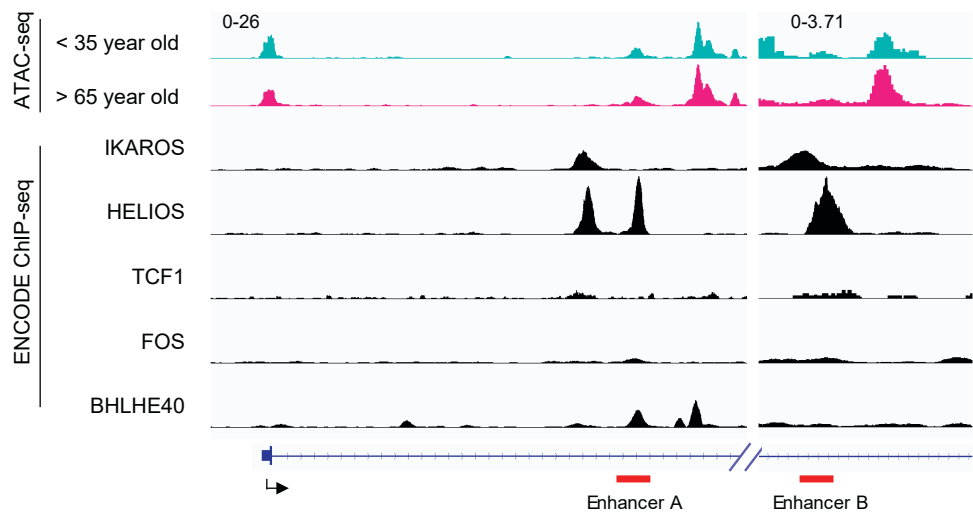


Figure S8, related to Figure 5. IKZF2 binding to *IL2RA* enhancers from ENCODE ChIP-seq.

A. ATAC-seq genome tracks of unstimulated naïve CD4⁺ T cells from young and older adults were aligned with ENCODE ChIP-seq genome tracks of indicated TFs at *IL2RA* enhancer locus (see Figure 5A). The location of enhancer A and enhancer B is indicated by red bars. **B.** *IKZF2* and *IL2RA* transcripts from sorted CD25⁺ and CD25⁻ naïve CD4⁺ T cells from 7 donors.

A



B

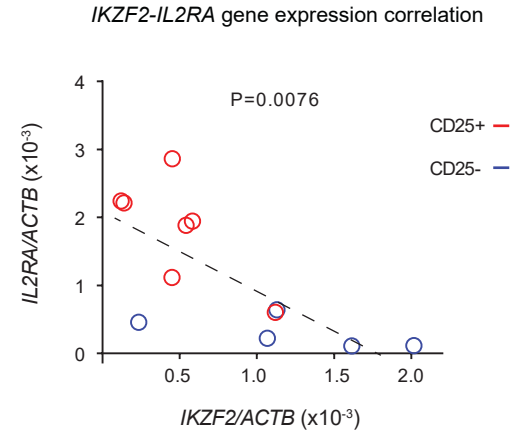
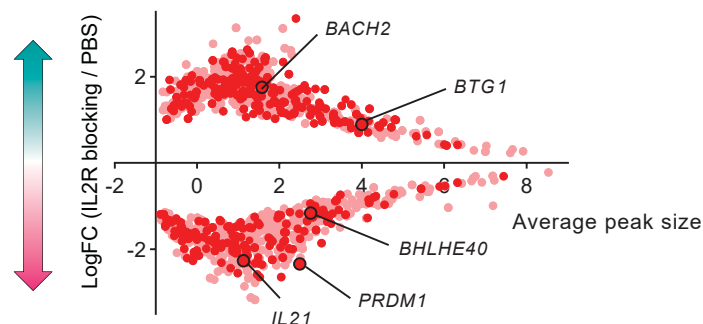


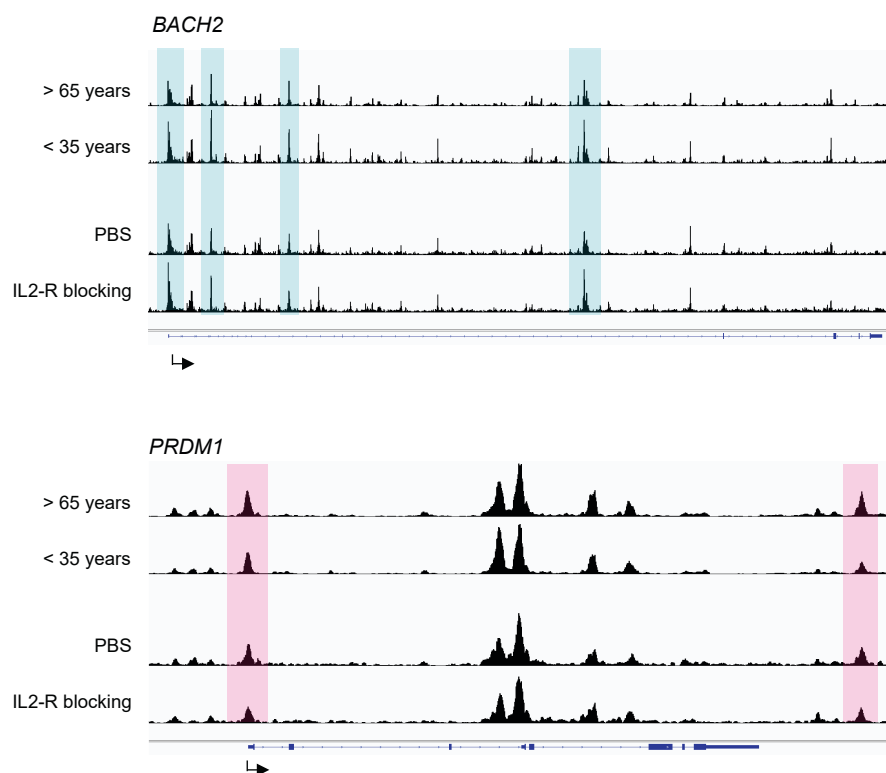
Figure S9, related to Figure 6. Genome accessibility changes induced by IL-2 receptor blocking.

A. LogFC of differential peaks between IL-2 receptor (IL-2R) blocking and PBS treatment ($p < 0.05$) are plotted against average peak size. Peaks that are also differentially accessible between young and older individuals are indicated in dark red. **B.** Accessibility tracks of representative genes. Magenta shaded areas indicate peaks that are more open in older adults and with PBS treatment; cyan indicate peaks that are more open in young adults and with IL-2R blocking treatment.

A



B



Supplement table 1. Study Population

Subject	Ethnicity	Gender	Age	Enrolled experiment
1	Caucasian	M	25	TCR-stimulation time course
2	Asian	F	70	TCR-stimulation time course
3	Caucasian	M	71	TCR-stimulation time course
4	Caucasian	F	30	TCR-stimulation time course
5	Asian	F	32	TCR-stimulation time course
6	Caucasian	M	65	TCR-stimulation time course
7	Caucasian	M	29	TCR-stimulation time course
8	Caucasian	M	74	TCR-stimulation time course
9	Caucasian	F	35	scMultiome
10	Asian	M	34	scMultiome
11	Caucasian	F	79	scMultiome
12	Caucasian	M	69	scMultiome
13	Caucasian	M	78	STAT5 inhibition ATAC-seq
14	Caucasian	F	80	STAT5 inhibition ATAC-seq
15	Caucasian	M	78	STAT5 inhibition ATAC-seq
16	Caucasian	F	81	STAT5 inhibition ATAC-seq

Supplement table 2. Antibodies

Antibody name	Clone	Supplier	Catalog #	Application
Anti-CD69 BV605	FN50	BioLegend	310937	Surface staining
Anti-CD25 BV421	BC96	BioLegend	302629	Surface staining
Anti-CD3 PE-Cy7	UCHT1	BioLegend	300420	Surface staining
Anti-CD4 AF700	RPA-T4	BioLegend	300526	Surface staining
Anti-CD45RA AF750	HI100	BioLegend	304151	Surface staining
Anti-CCR7 PerCP-Cy5.5	G043H7	BioLegend	353219	Surface staining
Anti-ZAP70 pY319 AF647	17A/P-ZAP70	BD	557817	Phosflow
Anti-SLP76 pY128 AF488	J141-668.36.58	BD	558439	Phosflow
Anti-ERK pT202 PE-CF594	20A	BD	562644	Phosflow
Anti-TCF1 PE	7F11A10	BioLegend	65520725	TF staining
Anti-BLIMP1 APC	646702	R&D systems	IC36081A	TF staining
Anti-IRF4	polyclonal	Cell Signaling	4964	Western blot
Anti-BHLHE40	Polyclonal	Novus Bio	NB100-1800	Western blot
Anti-β-actin	13E5	Cell Signaling	4970	Western blot
Anti-ERK pT202	D13.14.4E	Cell Signaling	4370	Western blot
Anti-LAT pY132	polyclonal	Invitrogen	44-224	Western blot
Anti-STAT5 pY694	polyclonal	Cell Signaling	9351	Western blot and ChIP
Anti-HELIOS	D8W4X	Cell Signaling	42427	Western blot and ChIP
Anti-CD25	BC96	BioLegend	302602	IL-2 receptor blocking
Anti-CD122	TU27	BioLegend	339002	IL-2 receptor blocking